

Regular article

Atomic electron-pair distances and subshell radii in position and momentum space*

Toshikatsu Koga, Hisashi Matsuyama

Department of Applied Chemistry, Muroran Institute of Technology, Muroran, Hokkaido 050-8585, Japan

Received: 8 April 1998 / Accepted: 6 July 1998 / Published online: 18 September 1998

Abstract. For the 53 neutral atoms from He to Xe in their ground states, the average distances $\langle u \rangle_{nl,n'l'}$ in position space and $\langle v \rangle_{nl,n'l'}$ in momentum space between an electron in a subshell nl and another electron in a subshell $n'l'$ are studied, where n and l are the principal and azimuthal quantum numbers of an atomic subshell, respectively. Analysis of 1700 subshell pairs shows that the electron-pair distances $\langle u \rangle_{nl,n'l'}$ in position space have an empirical but very accurate linear correlation with a one-electron quantity $U_{nl,n'l'} \equiv L_r + S_r^2/(3L_r)$, where L_r and S_r are the larger and smaller of subshell radii $\langle r \rangle_{nl}$ and $\langle r \rangle_{n'l'}$, respectively. The correlation coefficients are never smaller than 0.999 for the 66 different combinations of two subshells appearing in the 53 atoms. The same is also true in momentum space, and the electron-pair momentum distances $\langle v \rangle_{nl,n'l'}$ have an accurate linear correlation with a one-electron momentum quantity $V_{nl,n'l'} \equiv L_p + S_p^2/(3L_p)$, where L_p and S_p are the larger and smaller of average subshell momenta $\langle p \rangle_{nl}$ and $\langle p \rangle_{n'l'}$, respectively. Trends in the proportionality constants between $\langle u \rangle_{nl,n'l'}$ and $U_{nl,n'l'}$ and between $\langle v \rangle_{nl,n'l'}$ and $V_{nl,n'l'}$ are discussed based on a hydrogenic model for the subshell radial functions.

Key words: Two-electron intracule density – Electron-pair distance – Atomic subshell radius – Position space – Momentum space

1 Introduction

In atoms and atomic ions, the distribution of electrons around the nucleus is specified (see, e.g., [1, 2]) by the spherical average $\rho(r)$ of the spin-reduced one-electron

density function $\rho(\mathbf{r})$, where \mathbf{r} is the position vector of an electron and $r = |\mathbf{r}|$. The average electron-nucleus distance $\langle r \rangle$ follows immediately from $\rho(r)$ and characterizes the motion of electrons in an atomic system. Correspondingly, the distribution of electron momenta is determined (see, e.g., [2]) by the spherical average $\Pi(p)$ of the spin-reduced one-electron momentum density function $\Pi(\mathbf{p})$, where \mathbf{p} is the momentum vector of an electron and $p = |\mathbf{p}|$. The average momentum $\langle p \rangle$ follows from $\Pi(p)$ and characterizes the electronic motion from an alternative point of view.

In addition to the knowledge of the motion of a single electron, that of the relative motion of two electrons is important for a more profound understanding of the electronic structure of atoms. The relative motion of a pair of electrons in position space is described (see, e.g., [3–6]) by the intracule density $I(\mathbf{u})$ and its spherical averages $h(u)$, which are the probability density functions for the relative vector $\mathbf{r}_i - \mathbf{r}_j$ and its magnitude $|\mathbf{r}_i - \mathbf{r}_j|$ of any pair of electrons i and j to be \mathbf{u} and u , respectively. The corresponding intracule density and spherical average, $\bar{I}(\mathbf{v})$ and $\bar{h}(v)$, are introduced in momentum space and represent the probability densities for the relative momentum vector $\mathbf{p}_i - \mathbf{p}_j$ and its magnitude $|\mathbf{p}_i - \mathbf{p}_j|$ of any pair of electrons i and j to be \mathbf{v} and v , respectively. The average interelectronic distances $\langle u \rangle$ in position space and $\langle v \rangle$ in momentum space are obtained from the spherically averaged intracule densities $h(u)$ and $\bar{h}(v)$.

Even in atomic systems, the motion of any single electron around the coordinate origin and the relative motion of any pair of electrons are essentially different problems, and the associated one- and two-electron properties, such as the densities and the average distances, do not seem to have any definite relation. For the 53 neutral atoms from He to Xe we have recently examined [7, 8] the average interelectronic distance $\langle u \rangle_{nl}$ of a pair of electrons in an atomic subshell specified by the principal n and azimuthal l quantum numbers and found within the Hartree-Fock framework that $\langle u \rangle_{nl}$ has an accurate linear correlation with the average one-electron distance or subshell radius $\langle r \rangle_{nl}$. The same is true in momentum space, and the subshell interelec-

* Contribution to the Kenichi Fukui Memorial Issue

Correspondence to: T. Koga

tronic distance $\langle v \rangle_{nl}$ has been found to be proportional to the average one-electron momentum $\langle p \rangle_{nl}$ of that subshell. The proportionality constant in each space depends on the values of n and l .

In the present paper, we examine the average distances $\langle u \rangle_{nl,n'l'}$ in position space and $\langle v \rangle_{nl,n'l'}$ in momentum space between an electron in a subshell nl and another electron in a subshell $n'l'$ within the Hartree-Fock approximation. The 53 neutral atoms from He to Xe in their experimental ground states are the subject of this study, and hence there is a total of 1700 pairs of subshells nl and $n'l'$. Section 2 summarizes the definitions of one- and two-electron density functions, their subshell decompositions, and the associated average distances. In Sect. 3 we describe our computational procedures based on the numerical Hartree-Fock method. The results are presented and discussed in Sect. 4. From the analysis of the results of 1700 subshell pairs, it will be found that the electron-pair distances $\langle u \rangle_{nl,n'l'}$ in position space have a very accurate linear correlation with a one-electron quantity $U_{nl,n'l'} \equiv L_r + S_r^2/(3L_r)$, where L_r and S_r are the larger and smaller of subshell radii $\langle r \rangle_{nl}$ and $\langle r \rangle_{n'l'}$, respectively. Analogously, the electron-pair momentum distances $\langle v \rangle_{nl,n'l'}$ have an accurate linear correlation with a one-electron momentum-space quantity $V_{nl,n'l'} \equiv L_p + S_p^2/(3L_p)$, where L_p and S_p are the larger and smaller of average subshell momenta $\langle p \rangle_{nl}$ and $\langle p \rangle_{n'l'}$, respectively. Hartree atomic units are used throughout this paper.

2 Definitions

2.1 One-electron densities and subshell radii

For an N -electron system ($N \geq 1$), the spin-reduced one-electron density $\rho(\mathbf{r})$ and its spherical average $\rho(r)$ in position space are defined [1, 2, 9] by

$$\rho(r) \equiv N \int d\sigma dx_2 \dots dx_N |\Psi(x, x_2, \dots, x_N)|^2, \quad (1a)$$

$$\rho(r) \equiv (4\pi)^{-1} \int d\Omega_r \rho(\mathbf{r}), \quad (1b)$$

where $\mathbf{r} \equiv (r, \Omega_r)$ with $\Omega_r \equiv (\theta_r, \phi_r)$, $\Psi(x_1, \dots, x_N)$ is the electronic wave function of the system under consideration, and $x_i \equiv (\mathbf{r}_i, \sigma_i)$ is the combined position-spin coordinate of the electron i .

For a single Slater determinant Hartree-Fock wave function composed on N orthonormal spin-orbitals $\psi_j(\mathbf{r})\eta_j(\sigma)$, Eq. (1a) is rewritten as a sum of orbital contributions $|\psi_j(\mathbf{r})|^2$. For atoms and atomic ions, we can generally assume that the spatial function $\psi_j(\mathbf{r})$ has the form

$$\psi_j(\mathbf{r}) = R_{n,l_j}(r) Y_{l_j, m_j}(\Omega_r), \quad (2)$$

where $Y_{lm}(\Omega)$ is a spherical harmonic. The one-electron densities $\rho(\mathbf{r})$ and $\rho(r)$ for atoms are decomposed into contributions from different subshells specified by a set of the principal n and azimuthal l quantum numbers.

$$\rho(\mathbf{r}) = \sum_{nl} \rho_{nl}(\mathbf{r}), \quad \rho_{nl}(\mathbf{r}) = \sum_{j=1}^N \delta_{nn_j} \delta_{ll_j} |\psi_j(\mathbf{r})|^2, \quad (3a)$$

$$\rho(r) = \sum_{nl} \rho_{nl}(r), \quad \rho_{nl}(r) = (4\pi)^{-1} \sum_{j=1}^N \delta_{nn_j} \delta_{ll_j} |R_{n,l_j}(r)|^2, \quad (3b)$$

where δ_{ij} denotes the Kronecker delta. The average one-electron subshell distance $\langle r \rangle_{nl}$ is given by

$$\langle r \rangle_{nl} \equiv \int d\mathbf{r} r \rho_{nl}(\mathbf{r}) = 4\pi \int_0^\infty dr r^3 \rho_{nl}(r). \quad (3c)$$

The normalization of the subshell densities is

$$\int d\mathbf{r} \rho_{nl}(\mathbf{r}) = 4\pi \int_0^\infty dr r^2 \rho_{nl}(r) = N_{nl}, \quad (3d)$$

where N_{nl} is the number of electrons in the subshell nl . The reduced quantity $\langle r \rangle_{nl}/N_{nl}$ is hereafter referred to as the subshell radius.

If we start from a momentum-space N -electron wave function $\Phi(y_1, \dots, y_N)$, where $y_i \equiv (\mathbf{p}_i, \sigma_i)$ is the combined momentum-spin coordinate of electron i , an exactly analogous procedure defines the momentum-space one-electron density $\Pi(\mathbf{p})$ and its spherical average $\Pi(p)$. The Hartree-Fock wave function in momentum space has exactly the same determinantal structure as that in position space, provided that the one-electron spatial function $\psi_j(\mathbf{r})$ is replaced with

$$\phi_j(\mathbf{p}) = (2\pi)^{-3/2} \int d\mathbf{r} \exp(-i\mathbf{p} \cdot \mathbf{r}) \psi_j(\mathbf{r}). \quad (4a)$$

For the position-space atomic orbital given by Eq. (2), the corresponding momentum-space orbital is

$$\phi_j(\mathbf{p}) = P_{n,l_j}(p) Y_{l_j, m_j}(\Omega_p), \quad (4b)$$

where $\mathbf{p} \equiv (p, \Omega_p)$ and

$$P_{n,l_j}(p) = (-i)^{l_j} \sqrt{\frac{2}{\pi}} \int_0^\infty dr r^2 j_{l_j}(pr) R_{n,l_j}(r), \quad (4c)$$

in which $j_l(x)$ is the l th order spherical Bessel function of the first kind. The subshell components $\Pi_{nl}(\mathbf{p})$, $\Pi_{nl}(p)$, and $\langle p \rangle_{nl}$ in momentum space are obtained from equations analogous to Eqs. (3a)–(3c).

2.2 Intracule densities and intersubshell electron-pair distances

For an N -electron system ($N \geq 2$) the intracule density $I(\mathbf{u})$ and its spherical average $h(u)$ are defined [3, 4] by

$$I(\mathbf{u}) \equiv \int d\mathbf{r}_1 d\mathbf{r}_2 \delta[\mathbf{u} - (\mathbf{r}_1 - \mathbf{r}_2)] \Gamma(\mathbf{r}_1, \mathbf{r}_2), \quad (5a)$$

$$h(u) \equiv (4\pi)^{-1} \int d\Omega_u I(\mathbf{u}), \quad (5b)$$

where $\mathbf{u} \equiv (u, \Omega_u)$ with $\Omega_u \equiv (\theta_u, \phi_u)$, $\delta(\mathbf{r})$ is the three-dimensional Dirac delta function, and $\Gamma(\mathbf{r}_1, \mathbf{r}_2)$ is the spin-reduced two-electron density function [2, 9],

$$\Gamma(\mathbf{r}_1, \mathbf{r}_2) \equiv \left(\frac{N}{2} \right) \int d\sigma_1 d\sigma_2 dx_3 \dots dx_N |\Psi(x_1, \dots, x_N)|^2. \quad (6)$$

For a single Slater determinant wave function composed of N orthonormal spin-orbitals $\psi_j(\mathbf{r})\eta_j(\sigma)$, $\Gamma(\mathbf{r}_1, \mathbf{r}_2)$ reduces to a sum of spin-orbital-pair contributions,

$$\Gamma(\mathbf{r}_1, \mathbf{r}_2) = \frac{1}{2} \sum_{j=1}^N \sum_{k=1}^N \Gamma_{jk}(\mathbf{r}_1, \mathbf{r}_2), \quad (7a)$$

$$\Gamma_{jk}(\mathbf{r}_1, \mathbf{r}_2) = |\psi_j(\mathbf{r}_1)|^2 |\psi_k(\mathbf{r}_2)|^2 - \delta_s(j, k) \times [\psi_j^*(\mathbf{r}_1)\psi_k(\mathbf{r}_1)][\psi_k^*(\mathbf{r}_2)\psi_j(\mathbf{r}_2)], \quad (7b)$$

where $\delta_s(j, k)$ is unity if the two spin-orbitals j and k have the same spin and zero if they have opposite spins. Accordingly, the intracule densities $I(\mathbf{u})$ and $h(u)$ are decomposed into spin-orbital-pair components $I_{jk}(\mathbf{u})$ and $h_{jk}(u)$, respectively. When we use the kernel of three-dimensional Fourier transformations for the Dirac delta function,

$$\delta(\mathbf{r}) = (2\pi)^{-3} \int d\mathbf{s} \exp(+i\mathbf{r} \cdot \mathbf{s}), \quad (8)$$

the spin-orbital-pair components $I_{jk}(\mathbf{u})$ and $h_{jk}(u)$ are expressed [5, 10] as the Fourier and Hankel transforms of their characteristic functions $F_{jk}(\mathbf{s})$ and $H_{jk}(s)$,

$$I_{jk}(\mathbf{u}) = (2\pi)^{-3} \int d\mathbf{s} \exp(+i\mathbf{u} \cdot \mathbf{s}) F_{jk}(\mathbf{s}), \quad (9a)$$

$$h_{jk}(u) = (2\pi^2)^{-1} \int_0^\infty ds s^2 j_0(us) H_{jk}(s), \quad (9b)$$

where

$$F_{jk}(\mathbf{s}) \equiv F_{kk}^{jj}(\mathbf{s}) - \delta_s(j, k) F_{kj}^{kj}(\mathbf{s}), \quad (9c)$$

$$H_{jk}(s) \equiv H_{kk}^{jj}(s) - \delta_s(j, k) H_{kj}^{kj}(s), \quad (9d)$$

in which

$$F_{lm}^{jk}(\mathbf{s}) \equiv f_{jk}^*(\mathbf{s}) f_{lm}(\mathbf{s}), \quad \mathbf{H}_{lm}^{jk}(\mathbf{s}) \equiv (4\pi)^{-1} \int d\Omega_s \mathbf{F}_{lm}^{jk}(\mathbf{s}), \quad (9e)$$

$$f_{jk}(\mathbf{s}) \equiv \int d\mathbf{r} \exp(+i\mathbf{s} \cdot \mathbf{r}) \psi_j^*(\mathbf{r}) \psi_k(\mathbf{r}) = f_{kj}^*(-\mathbf{s}), \quad (9f)$$

and $\mathbf{s} \equiv (s, \Omega_s)$.

For atomic systems with the spatial function represented by Eq. (2) we obtain [5, 10]

$$f_{jk}(\mathbf{s}) = \sqrt{4\pi} \sum_{l=|j-k|}^{l_j+l_k} i^l \sqrt{2l+1} c^l(j; k) \times Y_{l, m_j - m_k}^*(\Omega_s) W_{ljk}(s), \quad (10a)$$

where

$$W_{ljk}(s) \equiv \int_0^\infty dr r^2 j_l(sr) R_j^*(r) R_k(r) = W_{ljk}^*(s), \quad (10b)$$

and $c^l(j; k) \equiv c^l(l_j m_j; l_k m_k)$ is the Condon-Shortley parameter [11]. Note that due to the property of $c^l(j; k)$, the summation in Eq. (10a) is over every other integer between the specified values. Based on Eq. (10a), the angular integration in the function $H_{lm}^{jk}(s)$ is performed analytically [10]. For the two components $H_{kk}^{jj}(s)$ and $H_{kj}^{kj}(s)$ appearing in Eq. (9d), we have [5, 10]

$$H_{kk}^{jj}(s) = \sum_{l=0}^{\min(2l_j, 2l_k)} (2l+1) a^l(j; k) w_{ljj}^*(s) W_{lkk}(s), \quad (11a)$$

$$H_{kj}^{kj}(s) = \sum_{l=|l_j-l_k|}^{l_j+l_k} (2l+1) b^l(k; j) |W_{ljk}(s)|^2, \quad (11b)$$

where $a^l(j; k) \equiv c^l(j; j) c^l(k; k)$ and $b^l(j; k) \equiv [c^l(j; k)]^2$ are Condon-Shortley parameters [11]. The summations in Eqs. (11a) and (11b) are over every other integer between the specified values.

The intersubshell intracule densities $I_{nl, n'l'}(\mathbf{u})$ and $h_{nl, n'l'}(u)$ are defined by

$$I_{nl, n'l'}(\mathbf{u}) = \frac{1}{2} \sum_{j=1}^N \sum_{k=1(k \neq j)}^N \delta_{nn_j} \delta_{ll_j} \delta_{n'n_k} \delta_{l'l_k} I_{jk}(\mathbf{u}), \quad (12a)$$

$$h_{nl, n'l'}(u) = \frac{1}{2} \sum_{j=1}^N \sum_{k=1(k \neq j)}^N \delta_{nn_j} \delta_{ll_j} \delta_{n'n_k} \delta_{l'l_k} h_{jk}(u), \quad (12b)$$

and the average intersubshell electron-pair distance $\langle u \rangle_{nl, n'l'}$ by

$$\begin{aligned} \langle u \rangle_{nl, n'l'} &\equiv \int d\mathbf{u} \mathbf{u} I_{nl, n'l'}(\mathbf{u}) \\ &= 4\pi \int_0^\infty du u^3 h_{nl, n'l'}(u). \end{aligned} \quad (12c)$$

The normalization of the intersubshell intracule densities is

$$\begin{aligned} \int d\mathbf{u} I_{nl, n'l'}(\mathbf{u}) &= 4\pi \int_0^\infty du u^2 h_{nl, n'l'}(u) \\ &= \begin{cases} N_{nl}(N_{nl} - 1)/2, & \text{if } n = n' \text{ and } l = l', \\ N_{nl} N_{n'l'}, & \text{if } n \neq n' \text{ or } l \neq l'. \end{cases} \end{aligned} \quad (12d)$$

Note that the intrasubshell densities $I_{nl, nl}(\mathbf{u})$ and $h_{nl, nl}(u)$ are meaningful only when there are two or more electrons in a subshell nl .

Exactly analogous definitions apply to the momentum-space intracule $\bar{I}(\mathbf{v})$ and $\bar{h}(v)$ densities, their subshell components, and the intersubshell electron-pair distances $\langle v \rangle_{nl, n'l'}$, if we start from a momentum-space N -electron wave function $\Phi(y_1, \dots, y_N)$, spin-orbitals $\phi_j(\mathbf{p})\eta_j(\sigma)$ and atomic radial functions $P_{n_l j}(p)$.

3 Computational details

Each atomic LS multiplet state is expressed in general by a linear combination of a finite number of Slater determinants in the Hartree-Fock theory, where L and S represent the total orbital and spin angular momentum quantum numbers, respectively. For the neutral atoms from He to Xe in their experimental ground states [12], we have previously confirmed [5] that among $(2L+1)(2S+1)$ degenerate states there exists at least one state with specific z -component M_L and M_S values of L and S that results in a single determinant wave function to which our mathematical procedure described in Sect. 2 can be applied.

For these ground multiplet states of the 53 neutral atoms expressed by single determinant wave functions, the Hartree-Fock radial functions $R_j(r) \equiv R_{n,l_j}(r)$ in position space were numerically generated using an enhanced and modified version of the MCHF72 code [13, 14]. The spherically averaged one-electron subshell density $\rho_{nl}(r)$ and the associated one-electron radius $\langle r \rangle_{nl}$ in position space were obtained straightforwardly. To obtain $W_{ljk}(s)$, products $R_j(r)R_k(r)$ of two radial functions were numerically Hankel-transformed using the algorithm of Talman [15]. Following Eqs. (9d), (11a) and (11b), we obtained the intersubshell components $H_{nl,n'l'}(s)$ of the characteristic function $H(s)$ as the selected sum of products of two $W_{ljk}(s)$ with appropriate coefficients. The Condon-Shortley parameters $a^l(j;k)$ and $b^l(j;k)$ were taken from Ref. [16]. An additional Hankel transformation [cf. Eq. (9b)] of the function $H_{nl,n'l'}(s)$ gave the intersubshell intracule density $h_{nl,n'l'}(u)$, from which the intersubshell electron-pair distance $\langle u \rangle_{nl,n'l'}$ was obtained.

For the determination of the corresponding one-electron subshell quantities $\Pi_{nl}(p)$ and $\langle p \rangle_{nl}$ and the two-electron intersubshell quantities $h_{nl,n'l'}(v)$ and $\langle v \rangle_{nl,n'l'}$ in momentum space, the position-space radial functions $R_j(r)$, generated by numerical Hartree-Fock calculations, were first Hankel-transformed to obtain the momentum-space radial functions $P_j(p) \equiv P_{n,l_j}(p)$ according to Eq. (4c). The same procedure was then applied as in position space.

4 Numerical results and discussion

By definition, all one-electron subshell density functions are normalized to the number of subshell electrons N_{nl} , while all two-electron intersubshell density functions are normalized to the number of electron pairs $N_{nl}(N_{nl}-1)/2$ or $N_{nl}N_{n'l'}$. Throughout this section, however, we will use a modified normalization scheme which normalizes all one-electron subshell and two-electron intersubshell densities to unity, in order to avoid large numbers and to facilitate mutual comparison of the one- and two-electron average distances.

For the Xe atom, Table 1 exemplifies the values of the average intersubshell electron-pair distances $\langle u \rangle_{nl,n'l'}$ in position space. Since Xe has 11 subshells, there are 66 pairs of subshells nl and $n'l'$, and the data are separated into four groups according to the values of $|n-n'|$ for

our later convenience. In Table 1, we find two trends of the $\langle u \rangle_{nl,n'l'}$ values: for given values of n and l , $\langle u \rangle_{nl,n'l'}$ increases with increasing n' , but is relatively insensitive to l' . We know that similar trends are observed for the atomic subshell radius $\langle r \rangle_{nl}$. The result suggests that the intersubshell electron-pair distances $\langle u \rangle_{nl,n'l'}$ have some meaningful correlation with the subshell radii $\langle r \rangle_{nl}$ and $\langle r \rangle_{n'l'}$ or their derivatives.

As a simple model, we consider classically that two electrons are moving independently on two concentric spheres with radii r_1 and r_2 , respectively. The average distance U between the two electrons is calculated to be

$$U = r_> + \frac{1}{3} \frac{r_<^2}{r_>}, \quad (13)$$

where $r_< \equiv \min(r_1, r_2)$ and $r_> \equiv \max(r_1, r_2)$. For an integer value of k , Sack [17] derived a general formula for the expansion of r_{12}^k in terms of r_1 , r_2 , and θ_{12} :

$$r_{12}^k = \sum_{l=0}^{\infty} g_{kl}(r_1, r_2) P_l(\cos \theta_{12}), \quad (14a)$$

where $P_l(x)$ is the Legendre polynomial and $g_{kl}(r_1, r_2)$ is an analytical function involving a hypergeometric function. A special case of Eq. (14a) for $k=1$ is

$$r_{12} = \sum_{l=0}^{\infty} \left(\frac{1}{2l+3} \frac{r_<^{l+2}}{r_>^{l+1}} - \frac{1}{2l-1} \frac{r_<^l}{r_>^{l-1}} \right) P_l(\cos \theta_{12}). \quad (14b)$$

U is identical to the leading term of Eq. (14b). When the expectation value of Eq. (14b) is examined over two spin-orbitals, however, we cannot obtain any relation between $\langle u \rangle_{nl,n'l'}$ and one-electron quantities because the radial integrands include $r_>$ and $r_<$. We then introduce a one-electron quantity $U_{nl,n'l'}$ defined by

$$U_{nl,n'l'} \equiv L_r + \frac{1}{3} \frac{S_r^2}{L_r}, \quad (15a)$$

as a quantum-mechanical analog of Eq. (13), where $S_r \equiv \min(\langle r \rangle_{nl}, \langle r \rangle_{n'l'})$ and $L_r \equiv \max(\langle r \rangle_{nl}, \langle r \rangle_{n'l'})$. For the particular case of $n=n'$ and $l=l'$, Eq. (15a) reduces to

$$U_{nl,nl} = \frac{4}{3} \langle r \rangle_{nl}, \quad (15b)$$

and the quantity $U_{nl,n'l'}$ is able to correctly predict accurate linear correlations reported [8] between $\langle u \rangle_{nl,nl}$ and $\langle r \rangle_{nl}$. In Table 1 the $U_{nl,n'l'}$ values for the Xe atom are summarized and compared with the $\langle u \rangle_{nl,n'l'}$ values. When the $U_{nl,n'l'}$ values are used to estimate the electron-pair distances $\langle u \rangle_{nl,n'l'}$, the relative errors Δ range from 0.0 to 12.2% and the heuristic one-electron quantity $U_{nl,n'l'}$ is seen to be a satisfactory approximation to the two-electron property $\langle u \rangle_{nl,n'l'}$. An interesting point is that the errors Δ are highly dependent on the $|n-n'|$ values. For $|n-n'|=0$ the relative error is 4.4–12.2%, but for $|n-n'|=1, 2, 3$ and 4 the errors are only about 2, 0.3, 0.04, and 0.00%, respectively. Namely, the accuracy of the approximation $\langle u \rangle_{nl,n'l'} \cong U_{nl,n'l'}$ increases as the difference between two subshell radii increases.

Stimulated by these results, we have examined possible correlations between $\langle u \rangle_{nl,n'l'}$ and $U_{nl,n'l'}$, based on the numerical Hartree-Fock data for the 1700 subshell

Table 1. Intersubshell electron-pair distances $\langle u \rangle_{nl, n'l'}$ and one-electron subshell quantities $U_{nl, n'l'}$ in position space for the Xe atom

$ n-n' $	nl	$n'l'$	$\langle u \rangle_{nl, n'l'}$	$U_{nl, n'l'}$	Δ	$ n-n' $	nl	$n'l'$	$\langle u \rangle_{nl, n'l'}$	$U_{nl, n'l'}$	Δ	
0	1s	1s	0.041064	0.037521	8.63	1	3d	4p	0.825805	0.810736	1.82	
	2s	2s	0.170717	0.161164	5.60		4d	4d	0.915303	0.900546	1.61	
		2p	0.170682	0.150176	12.01		4s	5s	2.109903	2.074419	1.68	
	2p	2p	0.147671	0.137443	6.93		5p	5p	2.446091	2.417173	1.18	
	3s	3s	0.446727	0.424928	4.88		4p	5s	2.120872	2.082554	1.81	
		3p	0.477162	0.418838	12.22			5p	2.456741	2.424065	1.33	
		3d	0.425712	0.400892	5.83		4d	5s	2.155927	2.108454	2.20	
	3p	3p	0.439137	0.412567	6.05			5p	2.491006	2.446010	1.81	
		3d	0.428556	0.394084	8.04							
	3d	3d	0.396587	0.373778	5.75		2	1s	3s	0.320248	0.319524	0.23
		4s	4s	1.040168	0.993690			4.47	3p	3p	0.311137	0.310279
	4s	4p	1.152916	1.015293	11.94			3d	3d	0.281856	0.281275	0.21
		4d	1.146506	1.083147	5.53		2s	4s	4s	0.755214	0.751802	0.45
	4p	4p	1.095921	1.036031	5.46			4p	4p	0.786732	0.783291	0.44
			4d	1.196345	1.101659		7.91	4d	4d	0.879104	0.876046	0.35
	4d	4d	1.229494	1.160602	5.60		2p	4s	4s	0.752679	0.750020	0.35
		5s	5s	2.762986	2.641278			4.40	4p	4p	0.784303	0.781582
	5s	5p	3.266537	2.897469	11.30		4d	4d	0.877130	0.874520	0.30	
		5p	5p	3.298940	3.117312		5.51	3s	5s	2.005104	1.998049	0.35
	1	1s	2s	0.125051	0.123057		1.59	3p	5p	2.358555	2.352465	0.26
2p			0.108449	0.105643	2.59	5s	2.003907		1.997070	0.34		
2s		3s	0.342141	0.333977	2.39	3d	5p	2.357645	2.351635	0.25		
		3p	0.333816	0.325165	2.59		5s	2.000094	1.994183	0.30		
		3d	0.305377	0.297706	2.51	5p	2.354398	2.349189	0.22			
2p		3s	0.335770	0.329810	1.77	3	1s	4s	0.745908	0.745622	0.04	
		3p	0.327557	0.320872	2.04		4p	4p	0.777664	0.777363	0.04	
3s		3d	0.300707	0.292968	2.57	4d	4d	0.870984	0.870755	0.03		
		4s	0.810180	0.790695	2.40	2s	5s	1.984590	1.983417	0.06		
4p		4p	0.838513	0.820594	2.14		5p	5p	2.341090	2.340067	0.04	
		4d	0.925778	0.909346	1.77	2p	5s	1.983683	1.982747	0.05		
3p		4s	0.805791	0.788091	2.20		5p	5p	2.340319	2.339499	0.04	
			4p	0.835756	0.818096	2.11						
		4d	0.923889	0.907116	1.82	4	1s	5s	1.981186	1.981092	0.00	
3d		4s	0.795181	0.780417	1.86		5p	5p	2.338180	2.338097	0.00	

pairs of the 53 atoms. We have found that there is good linear correlation between the two-electron property $\langle u \rangle_{nl, n'l'}$ and the one-electron property $U_{nl, n'l'}$ of the 53 atoms if the data are classified according to subshell pairs specified by the nl and $n'l'$ values. Table 2 summarizes the correlation coefficients (CCs) between $\langle u \rangle_{nl, n'l'}$ and $U_{nl, n'l'}$, together with the values of the parameter $a_{nl, n'l'}$ appearing in the least square linear approximation,

$$\langle u \rangle_{nl, n'l'} \cong a_{nl, n'l'} U_{nl, n'l'} . \quad (16)$$

In Table 2 we find that excellent correlations with $CC > 0.9999$ exist between $\langle u \rangle_{nl, n'l'}$ and $U_{nl, n'l'}$ for all subshell pairs with two exceptions, i.e. the $5p-5p$ and $4d-5s$ pairs, where $CC = 0.99985$ and 0.99975 , respectively. The CCs in Table 2 show a tendency to approach unity (i.e. perfect linearity) as $|n - n'|$ increases and we have $CC = 1.000000$ for all subshell pairs with $|n - n'| > 1$. Figure 1 depicts examples of the linear correlation for a few selected subshell pairs. In Table 2 the proportionality constants $a_{nl, n'l'}$ are distributed between 1.00 and 1.15 and do not differ much from one subshell pair to another. Moreover, the $a_{nl, n'l'}$ values tend to approach unity as $|n - n'|$ increases, as anticipated from the results for Xe in Table 1. It may be interesting to find the presence of an approximate but accurate linear relation

between the one-electron subshell property $U_{nl, n'l'}$ and the average electron-electron distance $\langle u \rangle_{nl, n'l'}$. When the $\langle u \rangle_{nl, n'l'}$ values are estimated from the $U_{nl, n'l'}$ values based on the regression line, Eq. (16), with the $a_{nl, n'l'}$ values in Table 2, the average relative error Δ_{av} for each subshell pair is largest for the $3d-3d$ pair with 1.31% among the 66 pairs. In most cases Δ_{av} is smaller than 0.5%, as shown in Table 2. Linear correlation between $\langle u \rangle_{nl, n'l'}$ and $U_{nl, n'l'}$ is concluded to be highly accurate though not rigorous.

The linearity observed above depends on the principal n and azimuthal l quantum numbers of two atomic subshells. To explain this fact, we have considered a hydrogenic radial function with an exponent $\zeta = Z/n$ with Z being nuclear charge,

$$R_{nl}(r) = (-1)^{n-l-1} 2^{\zeta/2} \left[\frac{(n-l-1)!}{n(n+l)!} \right]^{1/2} \times (2\zeta r)^l L_{n-l-1}^{2l+1}(2\zeta r) \exp(-\zeta r) , \quad (17)$$

where $L_n^k(x)$ is the associated Laguerre polynomial and the phase factor $(-1)^{n-l-1}$ is included for consistency through Eq. (4c) with the momentum-space counterpart which will be introduced later. A pair of hydrogenic functions, Eq. (17), predicts that the electron-pair distance $\langle u \rangle_{nl, n'l'}$ and the one-electron subshell property

Table 2. Linear correlations in position space between $\langle u \rangle_{nl,n'l'}$ and $U_{nl,n'l'}$. Note that all parent one-electron subshell and two-electron intersubshell densities are normalized to unity

$ n-n' $	Hartree-Fock						Hydrogenic							
	nl	$n'l'$	No. of pairs	CC	$a_{nl,n'l'}$	Δ_{av}	$ n-n' $	nl	$n'l'$	No. of pairs	CC	$a_{nl,n'l'}$	Δ_{av}	
0	1s	1s	53	0.999998	1.099201	0.36	1	3d	4p	24	0.999999	1.013875	0.25	
	2s	2s	51	0.999998	1.063783	0.32			4d	16	1.000000	1.010095	0.25	
	2p	2p	50	0.999996	1.150106	0.76		4s	5s	17	0.999992	1.011134	0.18	
	2p	2p	49	0.999987	1.091634	1.23			5p	6	1.000000	1.009064	0.16	
	3s	3s	43	0.999999	1.054136	0.17		4p	5p	17	0.999982	1.014282	0.17	
	3p	3p	42	0.999979	1.133719	0.52			5p	6	1.000000	1.010510	0.17	
	3d	3d	34	0.999961	1.065122	0.28		4d	5s	15	0.999752	1.030006	0.69	
	3p	3p	41	0.999979	1.071486	0.52			5p	6	0.999999	1.016441	0.13	
	3d	3d	34	0.999966	1.092110	0.28								
	3d	3d	33	0.999976	1.084568	1.31	2	1s	3s	44	1.000000	1.000734	0.09	
	4s	4s	33	0.999993	1.051731	0.31			3p	42	1.000000	1.000854	0.10	
		4p	24	0.999978	1.128082	0.47		2s	3d	34	1.000000	1.000878	0.06	
		4d	16	0.999975	1.047773	0.60			4s	36	1.000000	1.001337	0.13	
	4p	4p	23	0.999941	1.064986	0.55			4p	24	1.000000	1.001746	0.12	
	4d	4d	16	0.999957	1.074127	0.68		2p	4d	16	1.000000	1.001678	0.07	
	5s	5s	11	0.999979	1.071893	0.59			4s	36	1.000000	1.001138	0.10	
	5p	5p	6	0.999975	1.123407	0.26			4p	24	1.000000	1.001427	0.10	
	5p	5p	5	0.999852	1.065437	0.57		3s	5s	17	1.000000	1.001774	0.05	
	1	1s	2s	52	0.999999	1.007645	0.60		3p	5p	6	1.000000	1.001812	0.04
		2p	2p	50	0.999998	1.010589	1.07			5s	17	1.000000	1.001800	0.05
3s		3s	44	0.999994	1.011431	0.81			5p	6	1.000000	1.001803	0.04	
3p		3p	42	0.999997	1.011080	0.87		3d	5s	17	1.000000	1.001782	0.04	
		3d	34	0.999999	1.012929	0.64			5p	6	1.000000	1.001600	0.03	
2p		3s	44	0.999997	1.010990	0.44	3	1s	4s	36	1.000000	1.000097	0.01	
		3p	42	0.999998	1.010334	0.60			4p	24	1.000000	1.000141	0.01	
3s		3d	34	0.999999	1.012679	0.68			4d	16	1.000000	1.000123	0.01	
		4s	36	0.999997	1.010645	0.61		2s	5s	17	1.000000	1.000266	0.01	
4p		4p	24	0.999999	1.010937	0.56			5p	6	1.000000	1.000297	0.01	
4d		4d	16	1.000000	1.010050	0.33		2p	5s	17	1.000000	1.000217	0.01	
3p		4s	36	0.999995	1.012481	0.46			5p	6	1.000000	1.000239	0.01	
		4p	24	0.999998	1.011697	0.52	4	1s	5s	17	1.000000	1.000021	0.00	
4d		4d	16	1.000000	1.010366	0.33			5p	6	1.000000	1.000024	0.00	
3d		4s	34	0.999969	1.021674	0.35								

$U_{nl,n'l'}$ are proportional, and the proportionality constant is independent of Z but dependent on the four quantum numbers, electronic configurations, and LS

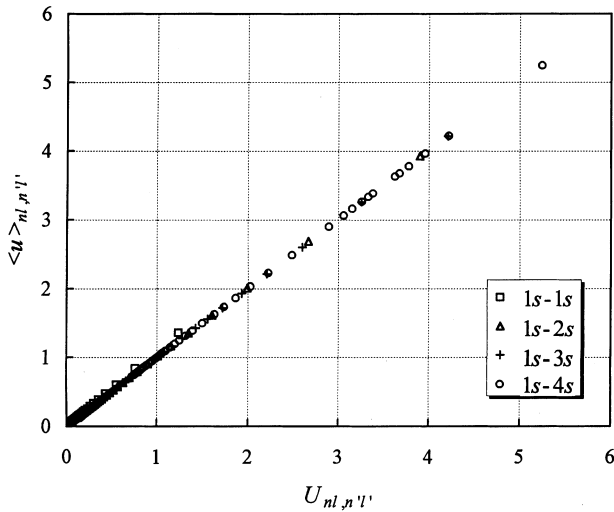


Fig. 1. Examples of the linear correlations observed in position space between $\langle u \rangle_{nl,n'l'}$ and $U_{nl,n'l'}$. Note that all the parent subshell and intersubshell densities are normalized to unity

coupling of electrons in relevant subshells. For pairs of closed $ns(2)$, $n'p(6)$, and $n''d(10)$ subshells with 1S coupling, we have evaluated the hydrogenic proportionality constants and tabulated them in Table 2. Comparison of the hydrogenic and Hartree-Fock $a_{nl,n'l'}$ values in Table 2 shows that the relative error of hydrogenic constants is at most 3.5%, and our hydrogenic model with the correct nodal structure of atomic subshells appears to explain semiquantitatively the observed linear correlations between $\langle u \rangle_{nl,n'l'}$ and $U_{nl,n'l'}$. However, the differences between the hydrogenic and Hartree-Fock constants are larger in general for a pair of outer subshells than for a pair of inner subshells.

The intersubshell electron-pair distances $\langle v \rangle_{nl,n'l'}$ in momentum space are summarized in Table 3 for the Xe atom. We can see from Table 3, that for given values of n and l , the electron-pair distance $\langle v \rangle_{nl,n'l'}$ decreases as n' increases. The subshell radius $\langle p \rangle_{nl}$ also decreases with increasing n in momentum space. The trend is exactly opposite to that which we have seen in position space due to the position-momentum reciprocity: an inner subshell with a tight electron density distribution around the nucleus ($\mathbf{r} = 0$) in position space has a diffuse density distribution in momentum space, while an outer subshell with a diffuse density in position space has a momentum density condensed around the momentum origin $\mathbf{p} = 0$.

Table 3. Intersubshell electron-pair distances $\langle v \rangle_{nl,n'l'}$ and one-electron subshell quantities $V_{nl,n'l'}$ in momentum space for the Xe atom

$ n-n' $	nl	$n'l'$	$\langle v \rangle_{nl,n'l'}$	$V_{nl,n'l'}$	Δ	$ n-n' $	nl	$n'l'$	$\langle v \rangle_{nl,n'l'}$	$V_{nl,n'l'}$	Δ
0	1s	1s	66.11437	60.40263	8.64	1	3d	4p	13.06400	12.39158	5.15
		2s	25.48414	21.79390	14.48			4d	12.95566	12.43204	4.04
	2p	2p	29.46985	26.12674	11.34	4s	5s	4.607850	4.148187	9.98	
		3s	13.07947	10.99588	15.93		5p	4.494404	4.145602	7.76	
	3p	3p	14.22833	12.17728	14.42	4p	5s	4.918076	4.558774	7.31	
		3d	15.41292	13.75590	10.75		5p	4.822722	4.556438	5.52	
	3d	3d	14.98250	13.17801	12.04	4d	5s	5.002363	4.713644	5.77	
		3d	16.12505	14.59117	9.51		5p	4.936156	4.711390	4.55	
	4s	3d	16.76650	15.78852	5.83	2	1s	3s	47.00206	45.80240	2.55
		4s	6.407826	5.327632	16.86			3p	47.28941	46.02073	2.68
	4p	4p	6.713185	5.624769	16.21	3d	4s	47.07563	46.33371	1.58	
		4d	6.672113	5.742481	13.93		4s	17.55979	16.67101	5.06	
	4d	4p	6.829005	5.894636	13.68	2p	4p	17.62701	16.74400	5.01	
		4d	6.903830	6.002941	13.05		4d	17.47074	16.77332	3.99	
	5s	4d	6.808747	6.107534	10.30	4p	4s	22.87734	22.33716	2.36	
		5s	2.183669	1.802514	17.45		4p	22.88726	22.39116	2.17	
	5p	5p	2.179716	1.794875	17.66	4d	4d	22.80214	22.41284	1.71	
		5p	2.064398	1.787172	13.43		3s	8.616127	8.320777	3.43	
	1	1s	2s	50.99083	47.26784	7.30	3p	5s	8.551507	8.319525	2.71
			2p	53.09924	48.89451	7.92		5p	10.15942	9.945147	2.11
2s		3s	20.25446	17.73238	12.45	3d	5s	10.10377	9.944102	1.58	
		3p	20.97990	18.33749	12.59		5p	12.04390	11.89284	1.25	
2p		3d	21.32249	19.20491	9.93	5p	5p	12.00500	11.89196	0.94	
		3s	24.71897	23.12230	6.46		3	1s	4s	45.79215	45.41945
3p		25.04899	23.56992	5.90	4p	45.81194			45.44579	0.80	
3s		3d	25.56132	24.21157	5.28	4d	4d	45.68556	45.45636	0.50	
		4s	10.23216	8.892232	13.10		2s	5s	16.55917	16.38269	1.07
3p		4p	10.30719	9.036902	12.32	5p	5p	16.51929	16.38206	0.83	
		4d	10.14104	9.094997	10.31		2p	5s	22.22607	22.12388	0.46
3d		4s	11.43623	10.42198	8.87	5p		5p	22.19816	22.12341	0.34
		4p	11.46822	10.54269	8.07		4	1s	5s	45.38140	45.31542
4d		11.38155	10.59116	6.94	5p	45.36546			45.31519	0.11	
4s		4s	13.00129	12.29082	5.46						

Since our classical model of two independent electrons moving on two concentric momentum spheres results in an expression isomorphic to Eq. (13) for the electron-pair momentum distance V , we introduce a momentum-space one-electron quantity $V_{nl,n'l'}$ defined by

$$V_{nl,n'l'} \equiv L_p + \frac{1}{3} \frac{S_p^2}{L_p}, \quad (18)$$

where $S_p \equiv \min(\langle p \rangle_{nl}, \langle p \rangle_{n'l'})$ and $L_p \equiv \max(\langle p \rangle_{nl}, \langle p \rangle_{n'l'})$. When $n = n'$ and $l = l'$, Eq. (18) simplifies to $V_{nl,nl} = (4/3)\langle p \rangle_{nl}$ and $V_{nl,n'l'}$ explains the linearity found previously [8] between $\langle v \rangle_{nl,nl}$ and $\langle p \rangle_{nl}$. In Table 3 the values of $V_{nl,n'l'}$ for the Xe atom are shown and compared them with the corresponding $\langle v \rangle_{nl,n'l'}$ values. When $V_{nl,n'l'}$ is employed as an approximation for $\langle v \rangle_{nl,n'l'}$, the relative errors Δ range from 0.1 to 16.9%. The errors tend to decrease as $|n - n'|$ increases as they do in position space. Though the accuracy is slightly poorer than that in position space, the one-electron subshell quantity $V_{nl,n'l'}$ can be used to estimate the electron-pair momentum distance $\langle v \rangle_{nl,n'l'}$.

We have examined correlations between $\langle v \rangle_{nl,n'l'}$ and $V_{nl,n'l'}$ for the 1700 subshell pairs of the 53 neutral atoms. The results are summarized in Table 4, where $b_{nl,n'l'}$ is the parameter appearing in the least square linear fitting,

$$\langle v \rangle_{nl,n'l'} \cong b_{nl,n'l'} V_{nl,n'l'}. \quad (19)$$

An excellent linear correlation is seen in Table 4, as was in position space. All the CCs between $\langle v \rangle_{nl,n'l'}$ and $V_{nl,n'l'}$ are larger than 0.9999, but we have eight exceptions when 4s or 5s subshells participate. Thus, the two-electron $\langle v \rangle_{nl,n'l'}$ and one-electron $V_{nl,n'l'}$ properties are essentially proportional. The proportionality constants $b_{nl,n'l'}$ in Table 4 range from 1.00 to 1.21 and show a tendency to approach unity with increasing $|n - n'|$. When Eq. (19) is employed to approximate $\langle v \rangle_{nl,n'l'}$ based on $V_{nl,n'l'}$, the average relative error Δ_{av} is largest (3.30%) for the 3s-4s subshell pair, but does not exceed 1% for many subshell pairs. The linear correlations observed in momentum space are illustrated in Fig. 2 for a few selected subshell pairs.

When momentum-space hydrogenic radial functions,

$$P_{nl}(p) = (-i)^l 2^{l+2} \zeta^{5/2} l! \left[\frac{2n(n-l-1)!}{\pi(n+l)!} \right]^{1/2} \times \frac{(2\zeta p)^l}{(p^2 + \zeta^2)^{l+2}} C_{n-l-1}^{l+1} \left(\frac{\zeta^2 - p^2}{\zeta^2 + p^2} \right), \quad (20)$$

with $C_n^k(x)$ being the Gegenbauer polynomial and $\zeta = Z/n$, are assumed for two closed subshells nl and $n'l'$, we find that the quantities $\langle v \rangle_{nl,n'l'}$ and $V_{nl,n'l'}$ are precisely proportional independent of Z . The hydrogenic proportionality constants $b_{nl,n'l'}$ are summarized in Table 4. When the two sets of proportionality constants in Table 4 are compared, we find that the Hartree-Fock results are approximately explained by the hydrogenic model. However, the difference between the corresponding two values is not small when outer subshells are concerned and the maximum relative error of the hydrogenic result amounts to 12.8% for the 3s-5p subshell pair.

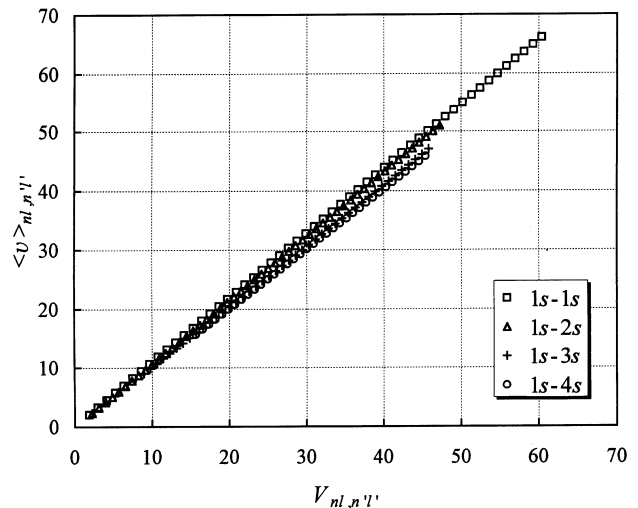


Fig. 2. Examples of the linear correlations observed in momentum space between $\langle v \rangle_{nl,n'l'}$ and $V_{nl,n'l'}$. Note that all the parent subshell and intersubshell densities are normalized to unity

5 Summary

We have studied the average distances $\langle u \rangle_{nl,n'l'}$ in position space and $\langle v \rangle_{nl,n'l'}$ in momentum space between an electron in a subshell nl and another electron in a subshell $n'l'$ of ground-state atoms. Analysis of 1700 subshell pairs of the 53 neutral atoms from He to Xe has shown that the electron-pair distances $\langle u \rangle_{nl,n'l'}$ in position space have an accurate linear correlation with a one-electron quantity $U_{nl,n'l'} \equiv L_r + S_r^2/(3L_r)$, where L_r and S_r are the larger and smaller of subshell radii $\langle r \rangle_{nl}$ and $\langle r \rangle_{n'l'}$, respectively. The correlation coefficients are greater than 0.9999 for 64 subshell pairs among a total of 66 pairs appearing in the 53 atoms. The momentum-space electron-pair distances $\langle v \rangle_{nl,n'l'}$ also have an accurate linear correlation with a one-electron momentum quantity $V_{nl,n'l'} \equiv L_p + S_p^2/(3L_p)$, where L_p and S_p are the larger and smaller of average subshell momenta $\langle p \rangle_{nl}$ and $\langle p \rangle_{n'l'}$, respectively. The correlation coefficients are again larger than 0.9999 for 58 subshell pairs of the total 66 pairs. Trends in the proportionality constants between $\langle u \rangle_{nl,n'l'}$ and $U_{nl,n'l'}$ and between $\langle v \rangle_{nl,n'l'}$ and $V_{nl,n'l'}$ can be roughly explained by assuming hydrogenic radial functions for the two relevant subshells.

Acknowledgements. This work has been supported in part by a Grant-in-Aid for Scientific Research from the Ministry of Education of Japan.

References

- Steiner E (1976) The determination and interpretation of molecular wave functions. Cambridge University Press, Cambridge, p 111ff
- Thakkar AJ, Tanner AC, Smith VH Jr (1987) In: Erdahl RM, Smith VH Jr (eds) Density matrices and density functionals. Reidel, Dordrecht, pp 327–337
- Coleman AJ (1967) Int J Quantum Chem Symp 1:457
- Thakkar AJ (1987) In: Erdahl RM, Smith VH Jr (eds) Density matrices and density functionals. Reidel, Dordrecht, pp 553–581

5. Koga T, Matsuyama H (1997) *J Chem Phys* 107:8510
6. Matsuyama H, Koga T, Romera E, Dehesa JS (1998) *Phys Rev A* 57:1759
7. Koga T, Matsuyama H, *J Mol Struct (Theochem)* (in press)
8. Koga T, Matsuyama H, *Theor Chem Acc* (in press)
9. Löwdin P-O (1955) *Phys Rev* 97:1474
10. Koga T, Matsuyama H, *J Phys B* (in press)
11. Condon EU, Shortley GH (1970) *The theory of atomic spectra*. Cambridge University Press, London, pp 175–176
12. Moore CE (1970) Ionization potentials and ionization limits derived from the analysis of optical spectra. NSRDS-NBS 34. National Bureau of Standards, Washington; (1971) Atomic energy levels. NSRDS-NBS 35, vols 1–3. National Bureau of Standards, Washington
13. Froese-Fischer C (1972) *Comput Phys Commun* 4:107
14. Froese-Fischer C (1977) *The Hartree-Fock method for atoms*. Wiley, New York
15. Talman JD (1983) *Comput Phys Commun* 30:93
16. Slater JC (1960) *Quantum theory of atomic structure*, vol 1. McGraw-Hill, New York, pp 488–490
17. Sack RA (1964) *J Math Phys* 5:245